Supplementary Material

Elovanoid-N34 is a homeostatic switch that modulates TXNRD1 for cell survival

Jorgelina M. Calandria, Surjyadipta Bhattacharjee, Sayantani Kala-Bhattacharjee, Pranab K. Mukherjee, Yuehan Feng, Jakob Vowinckel, Tobias Treiber and Nicolas G. Bazan*

*Correspondence: nbazan@lsuhsc.edu.

Running title: Elovanoid-N34 homeostatic switch modulates TXNRD1

Contents:

SUPPLEMENTARY FIGURES

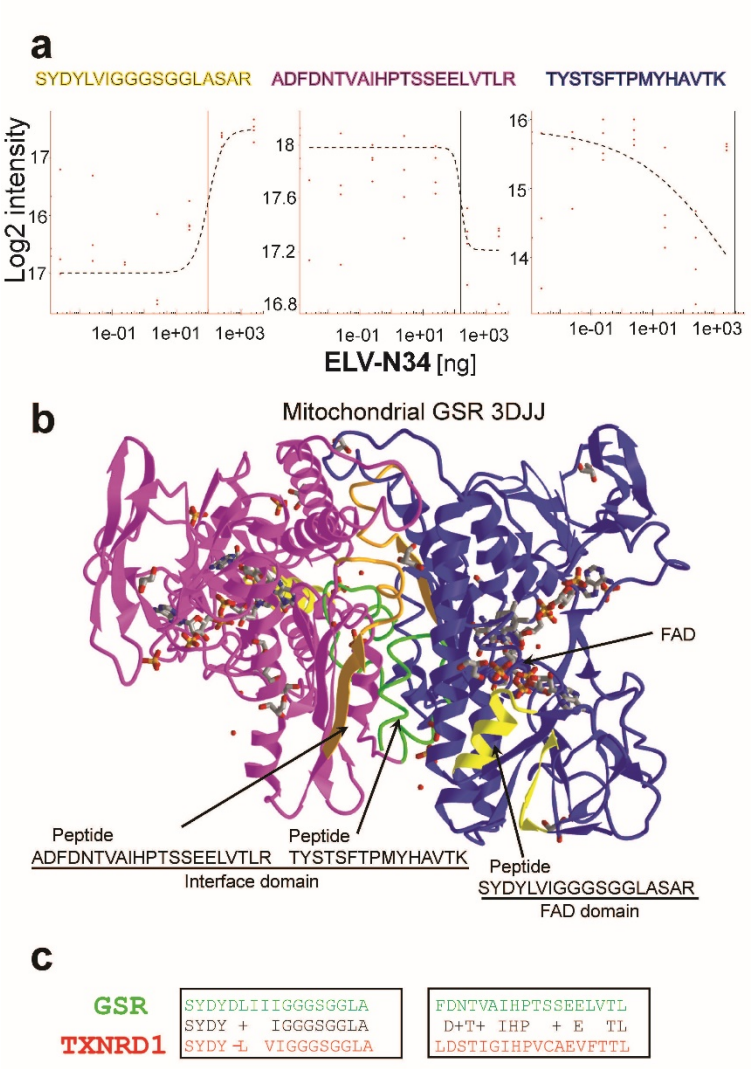

Fig. S1. Analysis of Target Candidate Protein Glutathione reductase, mitochondrial (GSR; P00390). The GSR displayed 3 peptides differentially proteolyzed in contact with ELV-N34. **a,** The plots show the peptide quantity vs. concentration of ELV-N34. The dotted line was determined by non-linear fit regression to obtain ED50 (vertical line). **b,** Structure shown is based on the X-ray chromatographic structure of human glutathione reductase (3DJJ), showing the 3D position of the peptides.

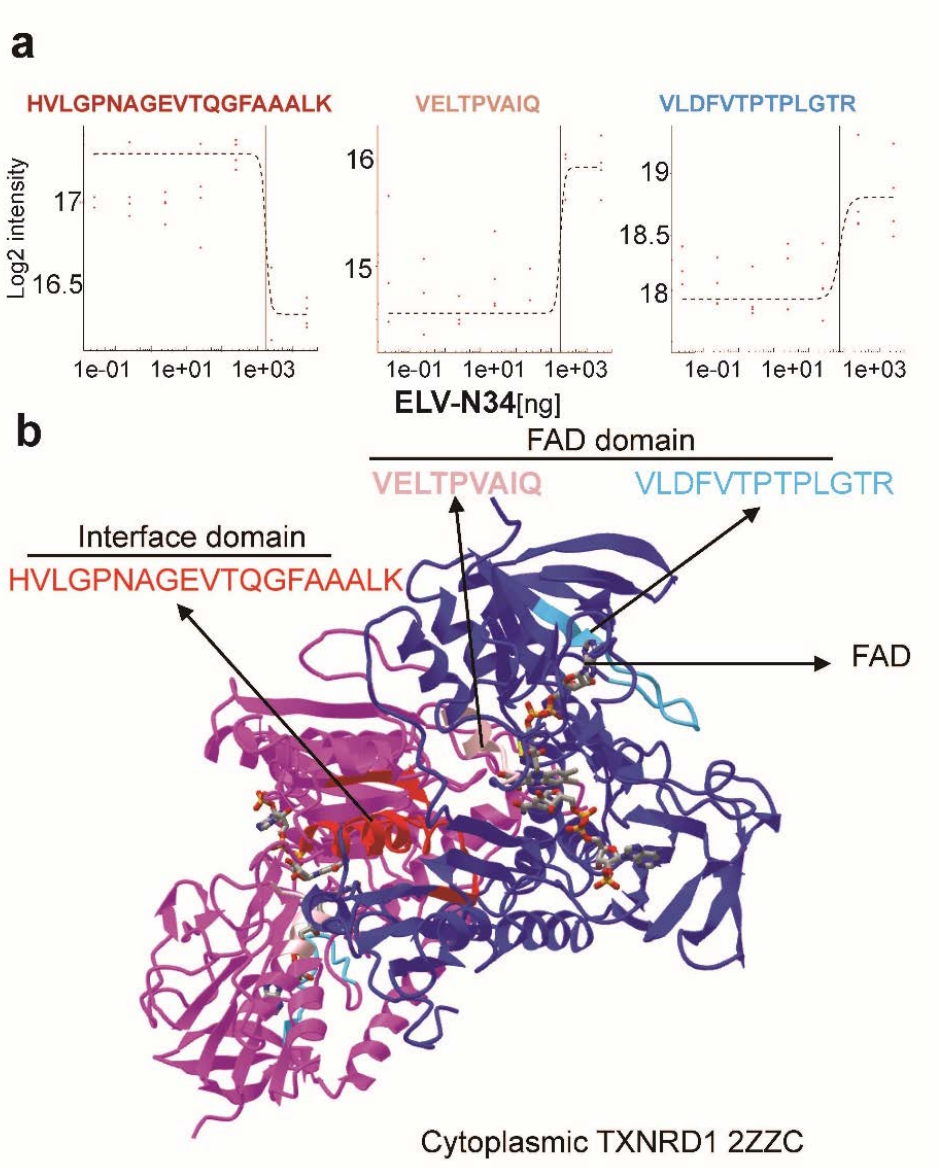

Fig. S2. Thioredoxin reductase, cytoplasmic (TXNRD1; Q16881). a, Plot shows the concentration curves for three of the 15 top quantified TXNRD1 peptides comparing DMSO and ELV-N34 treated samples. **b,** Highlighted peptides over the 3D ribbon model based on the X-ray crystallography (ID: 2ZZC).

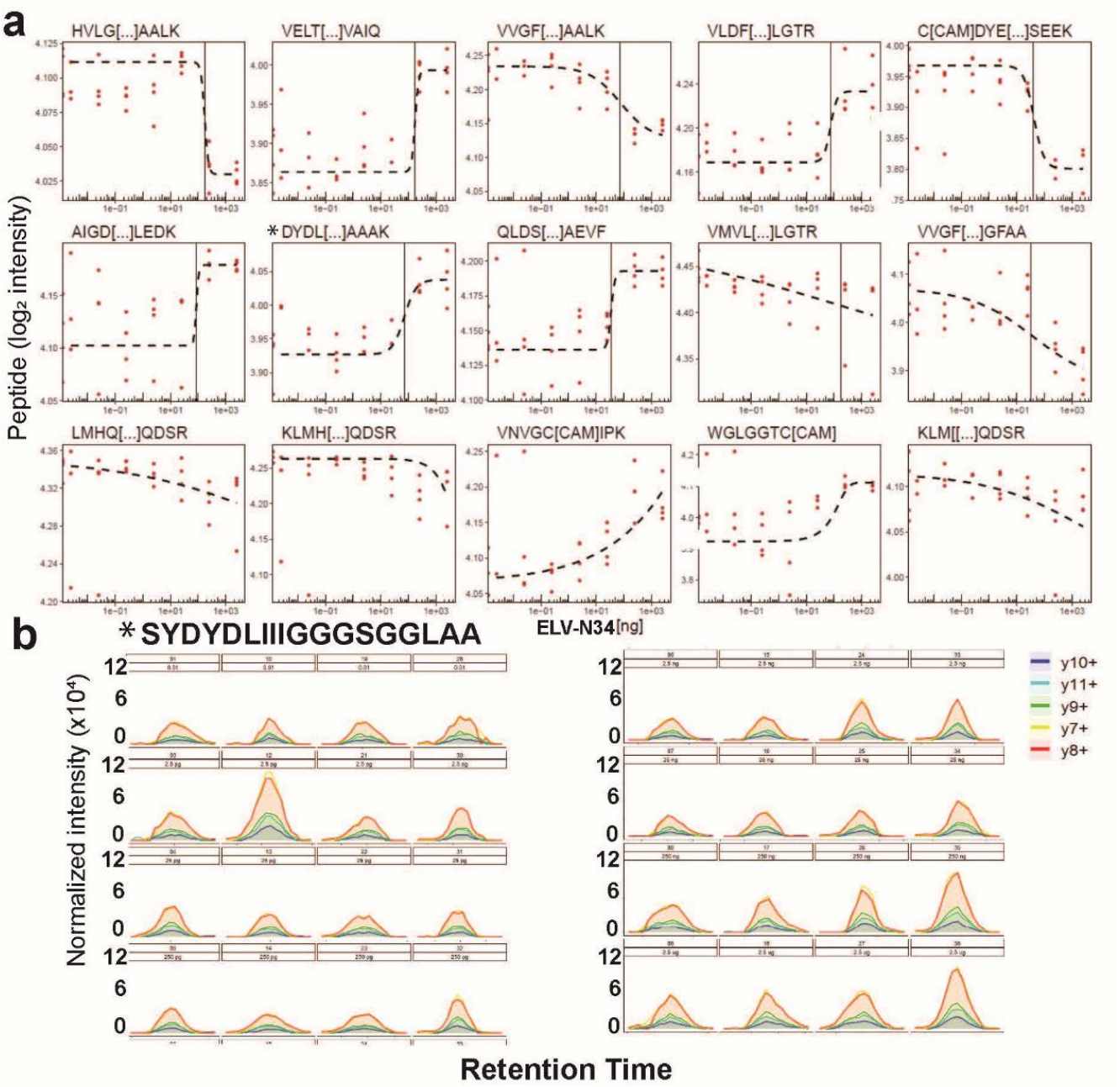

Fig. S3. Glutathione reductase (GSR; P00390). a, Plot shows changes of the top 15 quantified GSR peptides in DMSO and ELV-N34-treated samples. In the y-axis, the change is represented by log2 intensity, and the x-axis is the amount of ELV-N34 added in ng per reaction tested. Three peptides were significantly changed upon treatment with 250 nM ELV-N34 and used for

dose-response curve calculation. **b,** Extracted ion chromatogram plots show the response of peptide SYDYDLIIIGGGSGGLAA (blue, green, and red lines show three). With an asterisk, we marked the peptide in **a** and **b**.

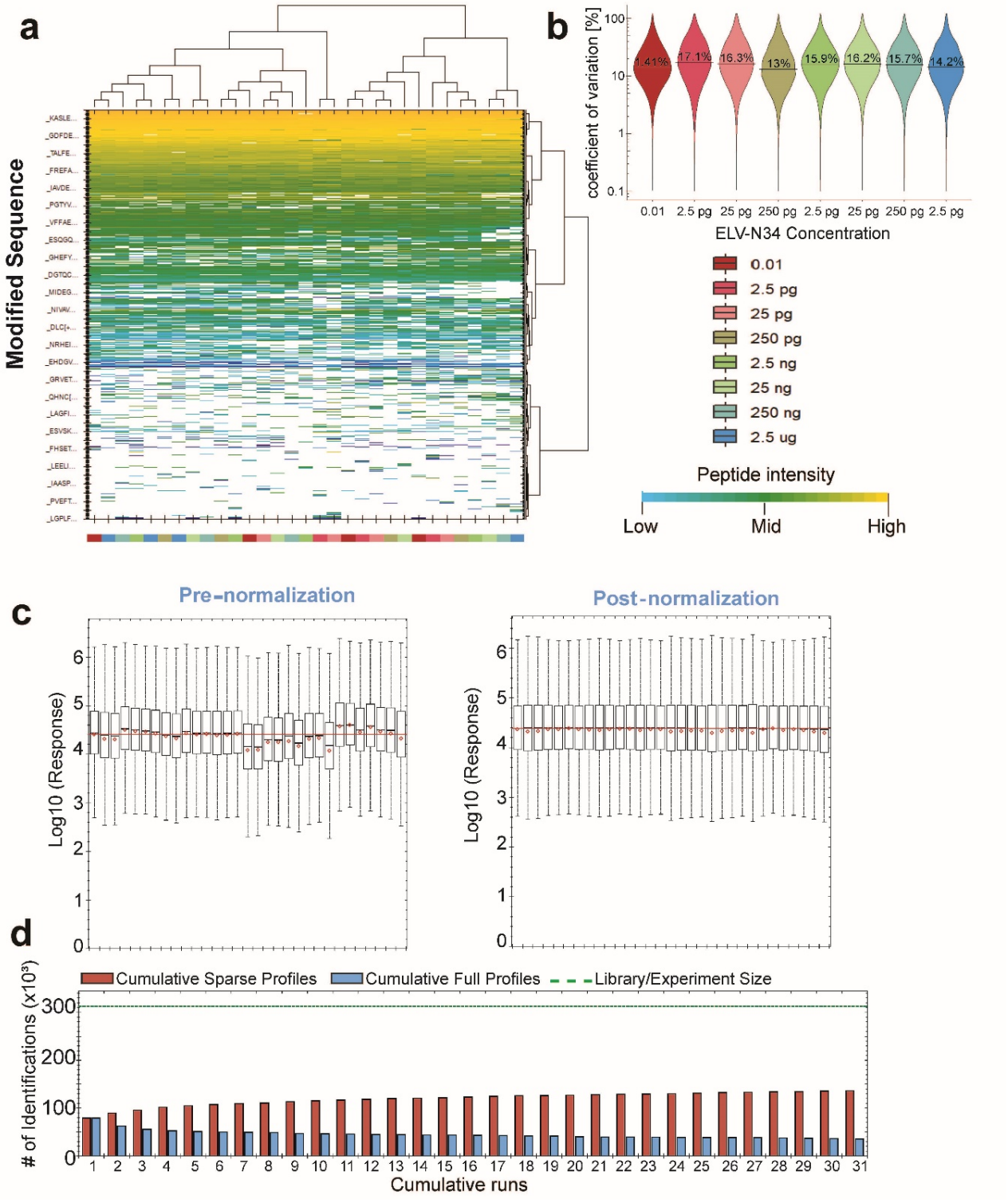
a
Modified Sequence
b
coefficient of variation [%]
100
10
1
0.1
1.41%
17.1%
16.3%
13%
15.9%
16.2%
15.7%
14.2%
0.01
2.5 pg
25 pg
250 pg
2.5 pg
25 pg
250 pg
2.5 pg
ELV-N34 Concentration
0.01
2.5 pg
25 pg
250 pg
2.5 ng
25 ng
250 ng
2.5 ug
Peptide intensity
Low
Mid
High
c
Pre-normalization
Post-normalization
Log10 (Response)
0
1
2
3
4
5
6
d
Cumulative Sparse Profiles
Cumulative Full Profiles
Library/Experiment Size
# of Identifications (x10³)
0
100
200
300
1 2 3 4 5 6 7 8 9 10 11 12 13 14 15 16 17 18 19 20 21 22 23 24 25 26 27 28 29 30 31
Cumulative runs

Fig. S4. Quality control of the first set of samples. a, Unsupervised clustering of 105’185 peptide intensities does not reconstruct sample groups. Hierarchical clustering analysis using the Manhattan distance measure using all peptide intensities across all samples was carried out. Clustered data is displayed as a heat map. Sample dendrogram (top) displays no separation according to sample group, indicating that no sample preparation or data acquisition artifact is confounding the analysis. **b,** Technical variation of target deconvolution experiment was assessed as coefficient of variance for peptide quantities between sample groups. Median technical variation was between 13.0 and 17.1 % within sample groups. Violin plot shows the distribution of coefficients of variation (CV) for peptide quantification, grouped by sample group. **c,** Minimal normalization was performed across all runs and was successful in reducing experimental variation. **d,** Number of precursors quantified across all runs. Data completeness is referred to as precursors quantified by HRM in the samples provided. Cumulative sparse profiles account for all precursors in the data set quantified at least once across the samples with high confidence (sparse data set). Cumulative full profiles account for all precursors in the data set quantified in each single sample with high confidence (complete data set). Size of the spectral library is shown as a dotted line.

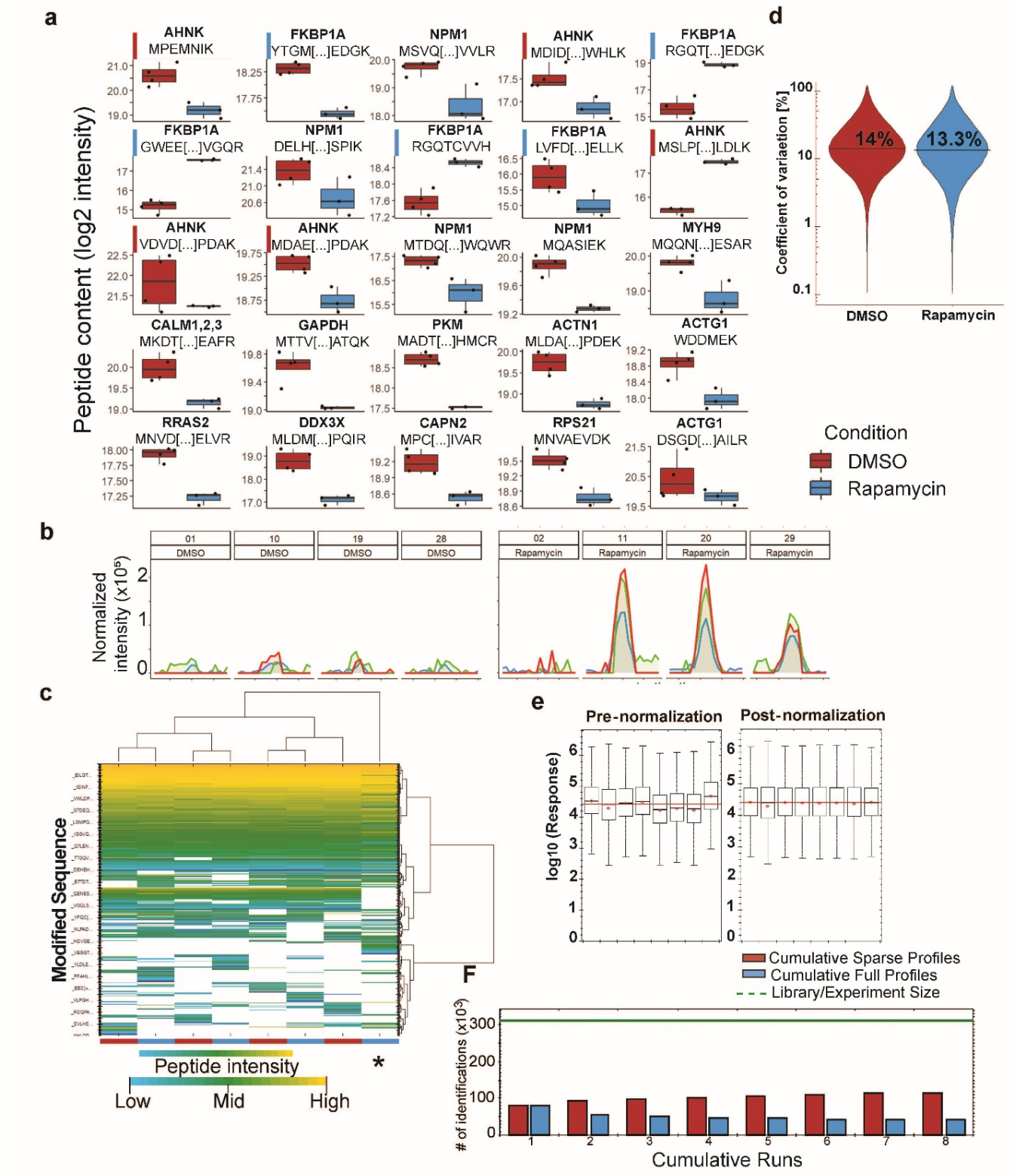

Fig. S5. Specificity control using Rapamycin instead of ELV-N34 for the first set of samples. The already known amount of 1’135 peptides was significantly changed between

samples treated with DMSO and Rapamycin. **a,** Box plot of the top 25 peptides and corresponding proteins significantly changed between DMSO and Rapamycin sample groups with 5 out of 25 high-ranking responder peptides. The candidate peptides shown were ranked by q-value. Data is grouped by sample groups and shown as box plots where the middle line depicts the average, and the limit of the boxes are the 1st and 3rd quartile. The bars show the standard deviation of the group. **b,** The known target of Rapamycin Peptidyl-prolyl cis-trans isomerase FKBP1A (FKBP1A; P62942). FKBP1A is identified, and extracted ion chromatogram plots show the response of peptide RGQTCVVHYTGMLEDGK^{2+}. **c,** Hierarchical Clustering (Rapamycin Control), unsupervised clustering of all peptide intensities does not reconstruct sample groups; the Manhattan distance measure using all peptide intensities across all samples was carried out. Clustered data is displayed as heat map. Sample dendrogram (top) displays no separation according to sample group, indicating that no sample preparation or data acquisition artifact is confounding the analysis. One sample (*) was excluded from analysis due to excessive variance. **d,** Technical variation: Median technical variation was between 13.3 and 14.0 % within sample groups. Violin plot shows distribution of coefficients of variance (CV) for peptide quantification, grouped by sample group. **e,** Normalization: Minimal normalization was performed across all runs and was successful in reducing experimental variation. **f,** Number of precursors quantified across all runs. Data completeness is referred to as precursors quantified by HRM in the samples provided. Cumulative sparse profiles account for all precursors in the data set quantified at least once across the samples with high confidence (sparse data set). Cumulative full profiles account for all precursors in the data set quantified in each single sample with high confidence (complete data set). Size of the spectral library is shown as dotted line.

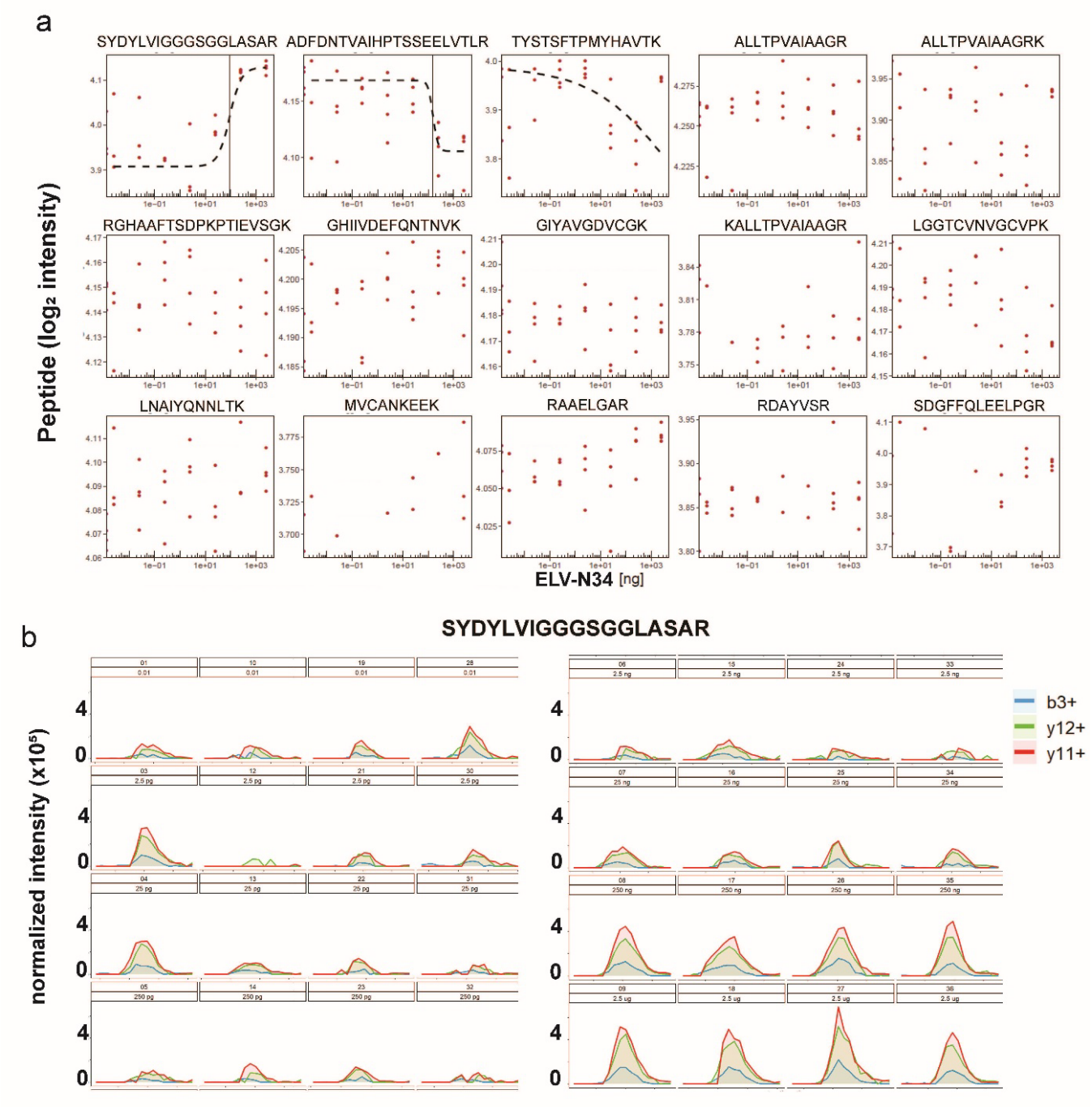

Fig. S6. a, Glutathione reductase, mitochondrial (GSR; P00390) peptides that appeared in the UOS + ELV-N34 LiP comparison. From the top 15 quantified GSR peptides in the comparison DMSO and ELV-N34 treated samples, 3 peptides were significantly changed upon treatment

with 250 ng ELV-N34 and used for dose-response curve calculation. **b,** XIC plots show response of peptide SYDYLVIGGGSGGLASAR.

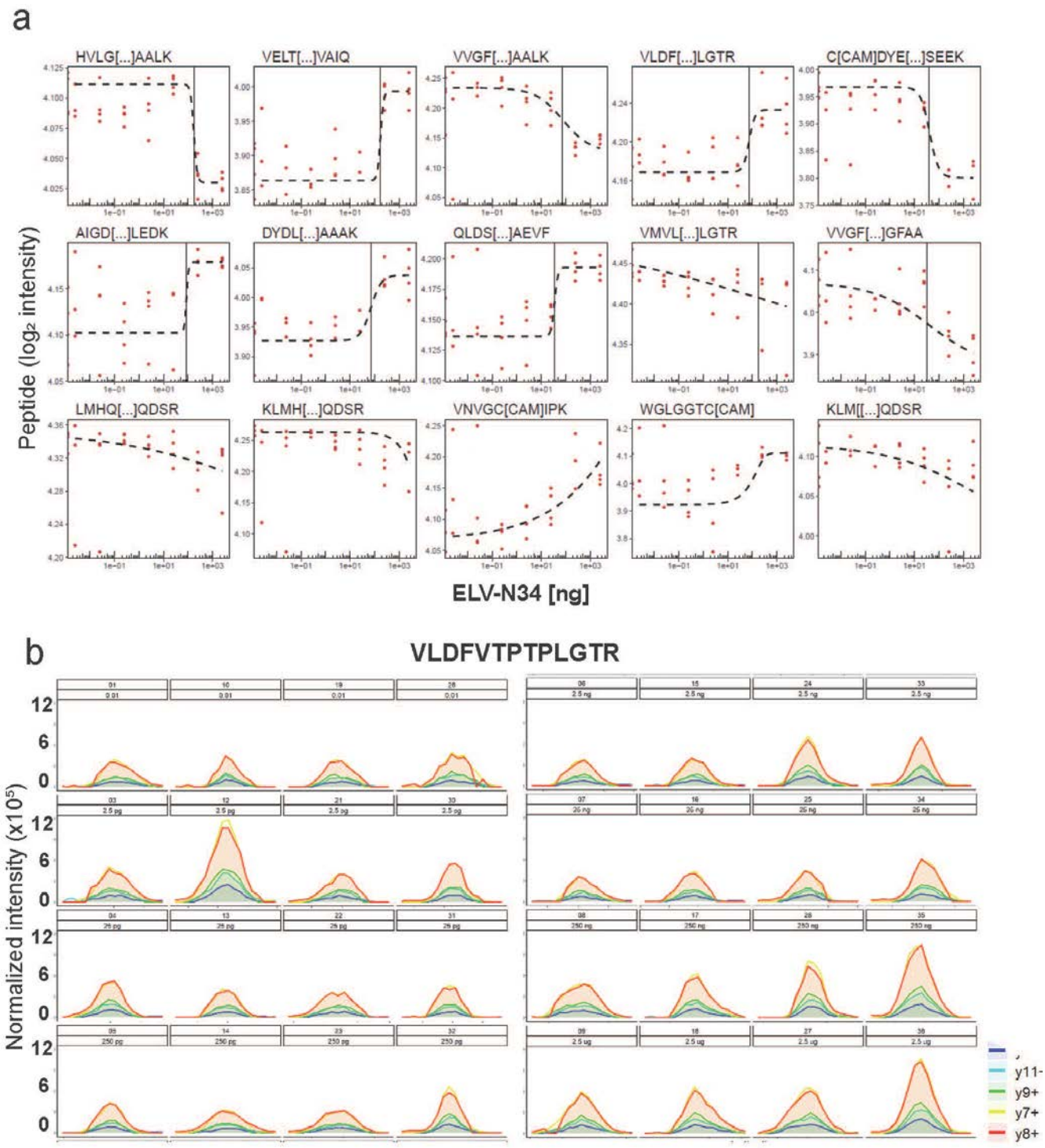
a
HVLG[...]AALK
VELT[...]VAIQ
VVGF[...]AALK
VLDF[...]LGTR
C[CAM]DYE[...]SEEK
AIGD[...]LEDK
DYDL[...]AAAK
QLDS[...]AEVF
VMVL[...]LGTR
VVGF[...]GFAA
LMHQ[...]QDSR
KLMH[...]QDSR
VNVGC[CAM]IPK
WGLGGTC[CAM]
KLM[[...]QDSR
Peptide (log2 intensity)
ELV-N34 [ng]
b
VLDFVTPTPLGTR
Normalized intensity (x10^5)
y11-
y9+
y7+
y8+

Fig. S7. Thioredoxin reductase 1, cytoplasmic (TXNRD1; Q16881). a, The plots show the fold change of the top 15 quantified TXNRD1 peptides in DMSO and ELV-N34 treated samples. More than 15 peptides were significantly changed upon treatment with 250 nM ELV-N34 and used for dose-response curve calculation. **b,** XIC plots show response of peptide VLDFVTPTPLGTR.

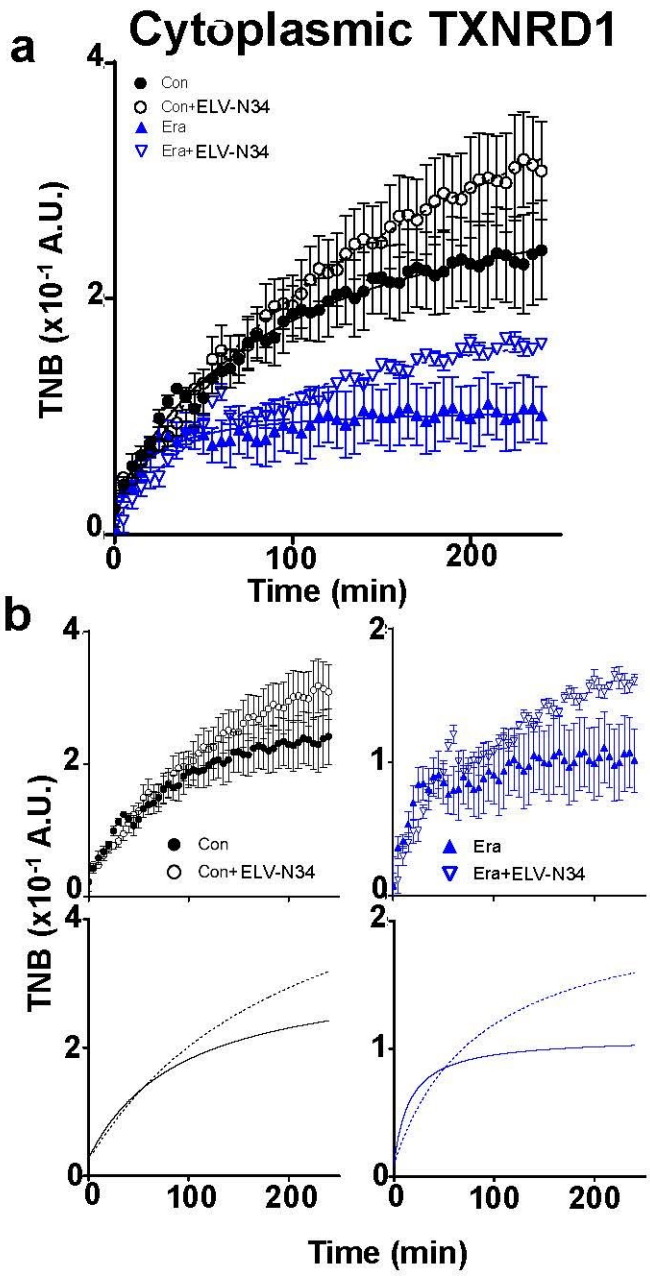

Fig. S8. Addition of ELV-N34 to the membrane and cytosolic fractions. Curves of Product vs. Time. **a-e,** 250 ng of ELV-N34 per 100 ng of cytoplasmic protein in 200 µl reaction was added to cytosolic (**a, b**), and membrane (**c, d**) fractions of ABC cells exposed to Erastin or

naïve, the activity of TXNRD1 was recorded as Product (absorbance at 412 nm) vs. Time (min), and the subtraction resulting from the reaction and the reaction plus inhibitor was plotted.

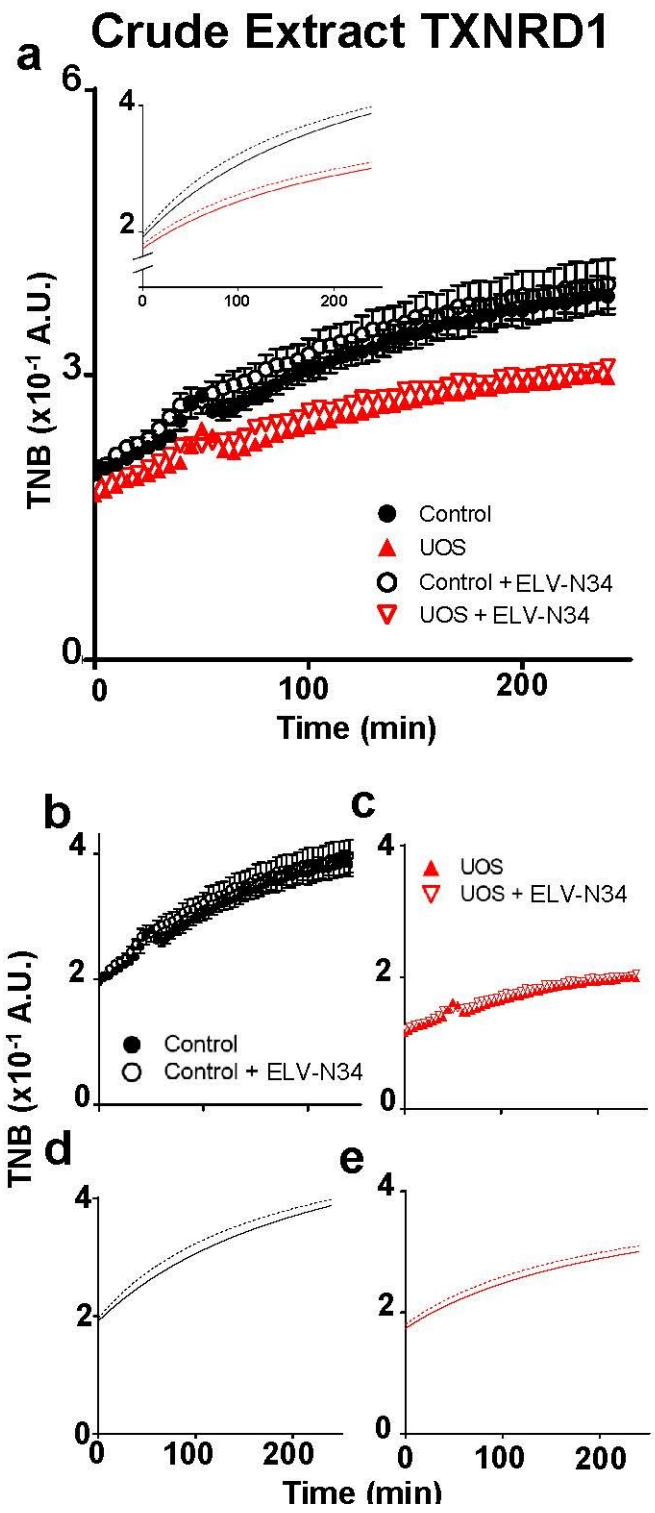
Crude Extract TXNRD1
a
TNB (x10-1 A.U.)
Time (min)
Control
UOS
Control + ELV-N34
UOS + ELV-N34
b
c
d
e

Fig. S9. Curves of Product vs. Time of the crude extract. a-e, 200 nM ELV-N34 was added to the ABC cells exposed to UOS or naïve. The activity of TXNRD1 was recorded on the total extract of the cells exposed to the mentioned treatments as Product (absorbance at 412 nm) vs. Time (min). Spureus reductase activity was ruled out using a specific inhibitor of TXNRD1. **a,** Merge curves of the four conditions. **b, c,** Mean of three observations and the bars represent the standard error of the mean for Control and Control + ELV-N34 (**b**) and UOS and UOS + ELV-N34 (**c**). **d, e,** The non-linear regression curves obtained for the data points in **b** and **c**.

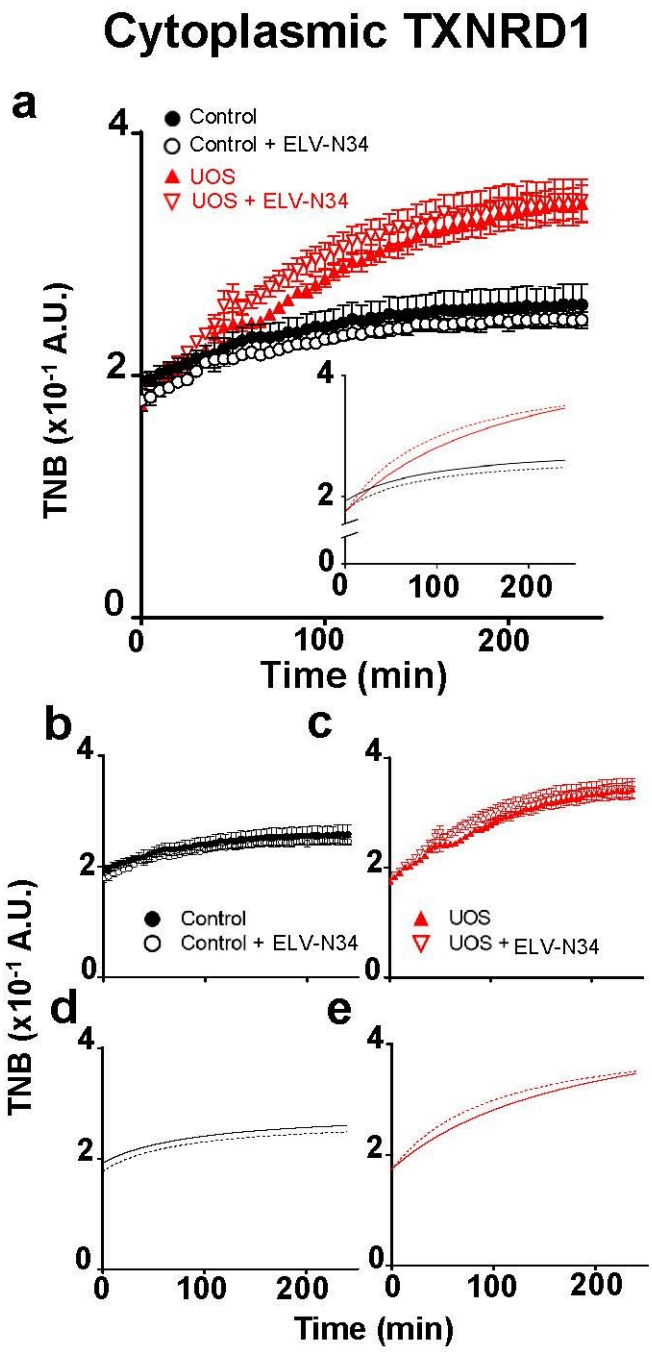

Fig. S10. Curves of Product vs. Time of the cytosolic TXNRD1. a-e, 200 nM ELV-N34 was added to the ABC cells exposed to UOS or naïve. The activity of TXNRD1 was recorded on the cytoplasmic fraction of the cells exposed to the mentioned treatments as product (absorbance at 412 nm) vs. Time (min). Spureus reductase activity was ruled out using a specific inhibitor of

TXNRD1. **a,** Merge curves of the four conditions. **b, c,** Mean of three observations and the bars represent the standard error of the mean for Control and Control + ELV-N34 (**b**) and UOS and UOS + ELV-N34 (**c**). **d, e,** The non-linear regression curves obtained for the data points in **b** and **c**.

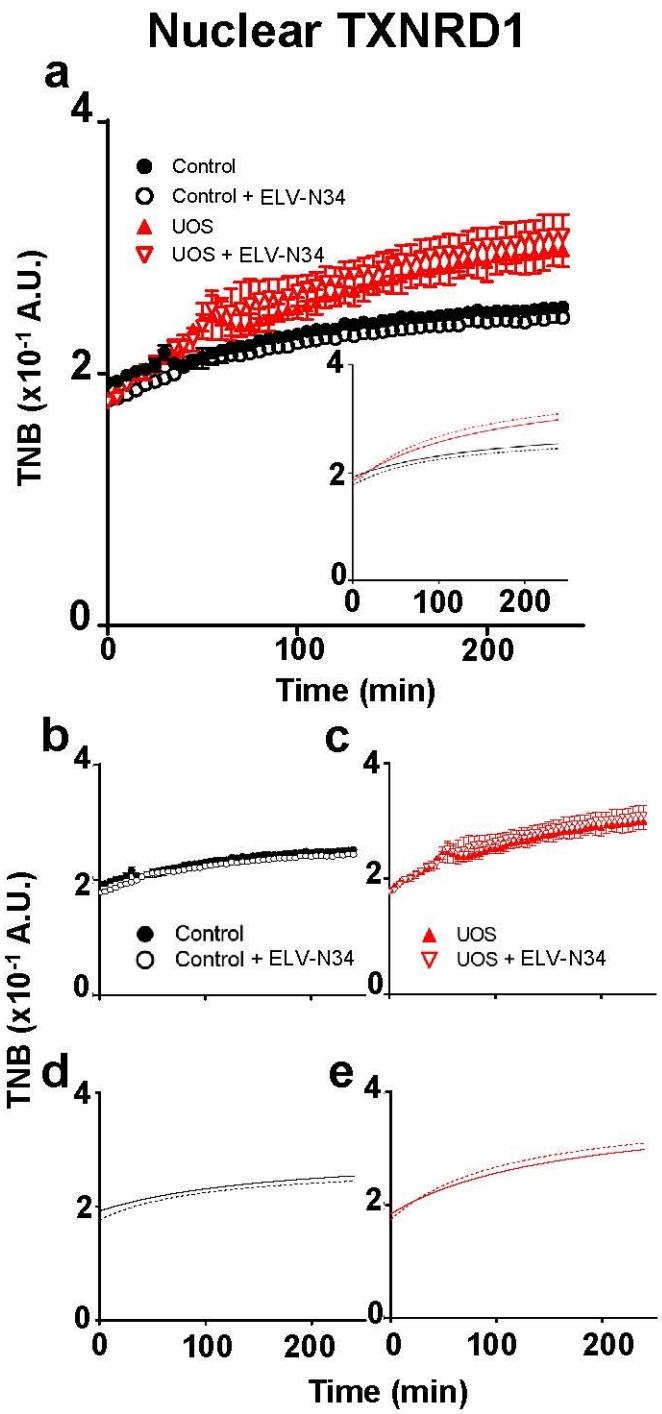

Fig. S11. Curves of Product vs. Time of the nuclear TXNRD1. a-e, 200 nM ELV-N34 was added to the ABC cells exposed to UOS or naïve. The activity of TXNRD1 was recorded on the

nuclear fraction of the cells exposed to the mentioned treatments as Product (absorbance at 412 nm) vs. Time (min). Spureus reductase activity was ruled out using a specific inhibitor of TXNRD1. **a,** Merge curves of the four conditions. **b, c,** Mean of three observations and the bars represent the standard error of the mean for Control and Control + ELV-N34 (**b**) and UOS and UOS + ELV-N34 (**c**). **d, e,** The non-linear regression curves obtained for the data points in **b** and **c**.

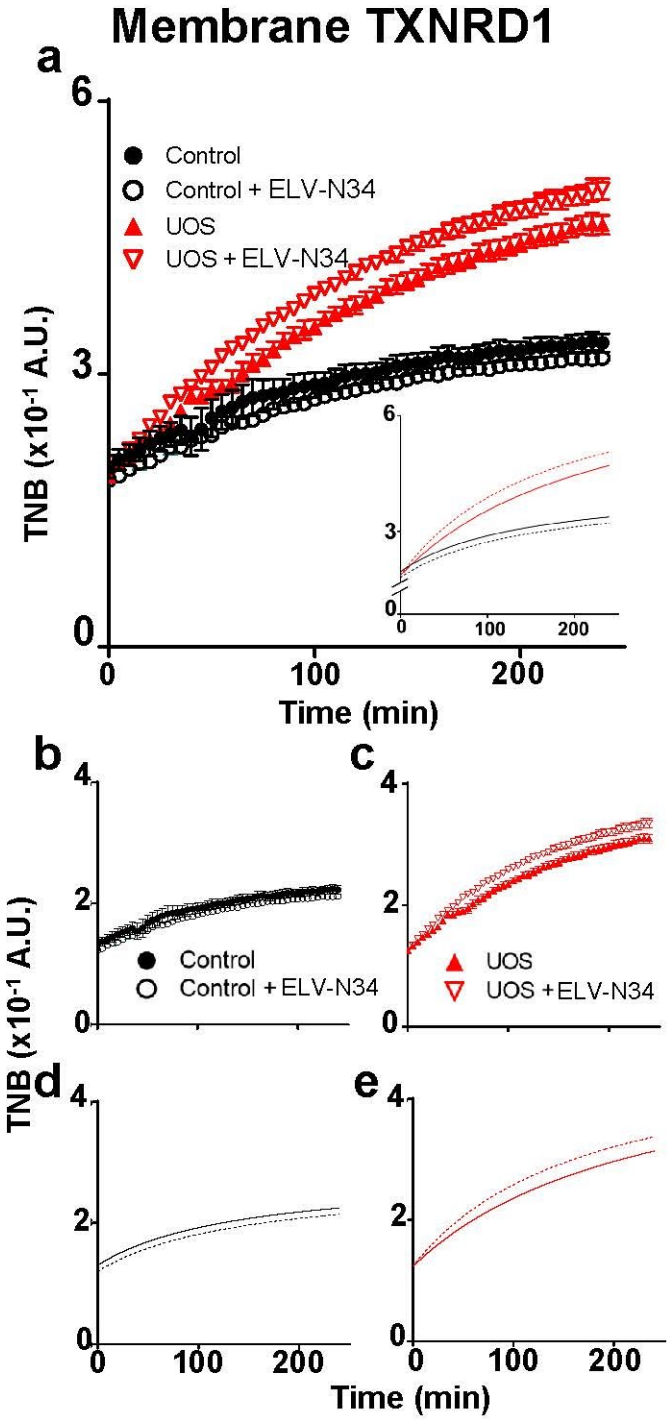

Fig. S12. Curves of Product vs. Time of the membrane TXNRD1. a-e, 200 nM ELV-N34 was added to the ABC cells exposed to UOS or naïve. The activity of TXNRD1 was recorded on the

membrane fraction of the cells exposed to the mentioned treatments as Product (absorbance at 412 nm) vs. Time (min). Spureus reductase activity was ruled out using a specific inhibitor of TXNRD1. **a,** Merge curves of the four conditions. **b, c,** Mean of three observations and the bars represent the standard error of the mean for Control and Control + ELV-N34 (**b**) and UOS and UOS + ELV-N34 (**c**). **d, e,** The non-linear regression curves obtained for the data points in **b** and **c**.

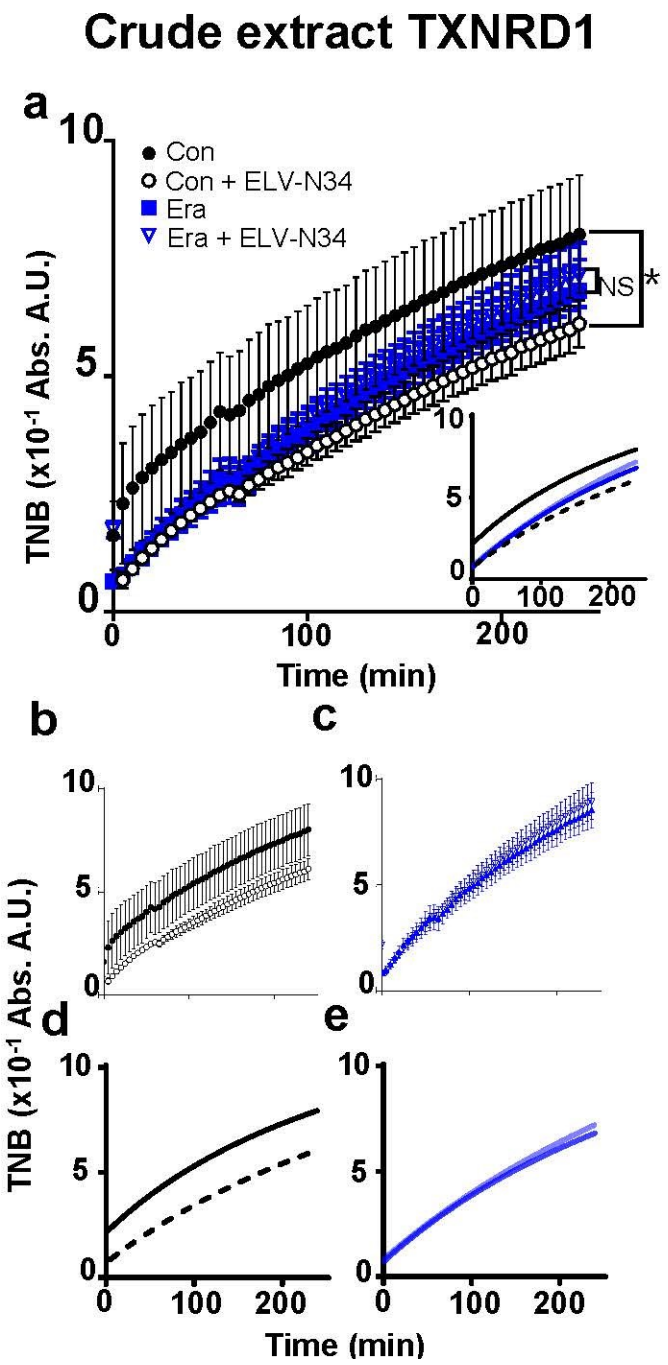

Fig. S13. Curves of Product vs. Time of the crude extract. a-e, 200 nM ELV-N34 was added to the ABC cells exposed to Erastin or naïve. The activity of TXNRD1 was recorded on the total extract of the cells exposed to the mentioned treatments as Product (absorbance at 412 nm) vs.

Time (min). Spureus reductase activity was ruled out using a specific inhibitor of TXNRD1. **a,** Merge curves of the four conditions. **b, c,** Mean of three observations and the bars represent the standard error of the mean for Control and Control + ELV-N34 (**b**) and UOS and UOS + ELV-N34 (**c**). **d, e,** The non-linear regression curves obtained for the data points in **b** and **c**.

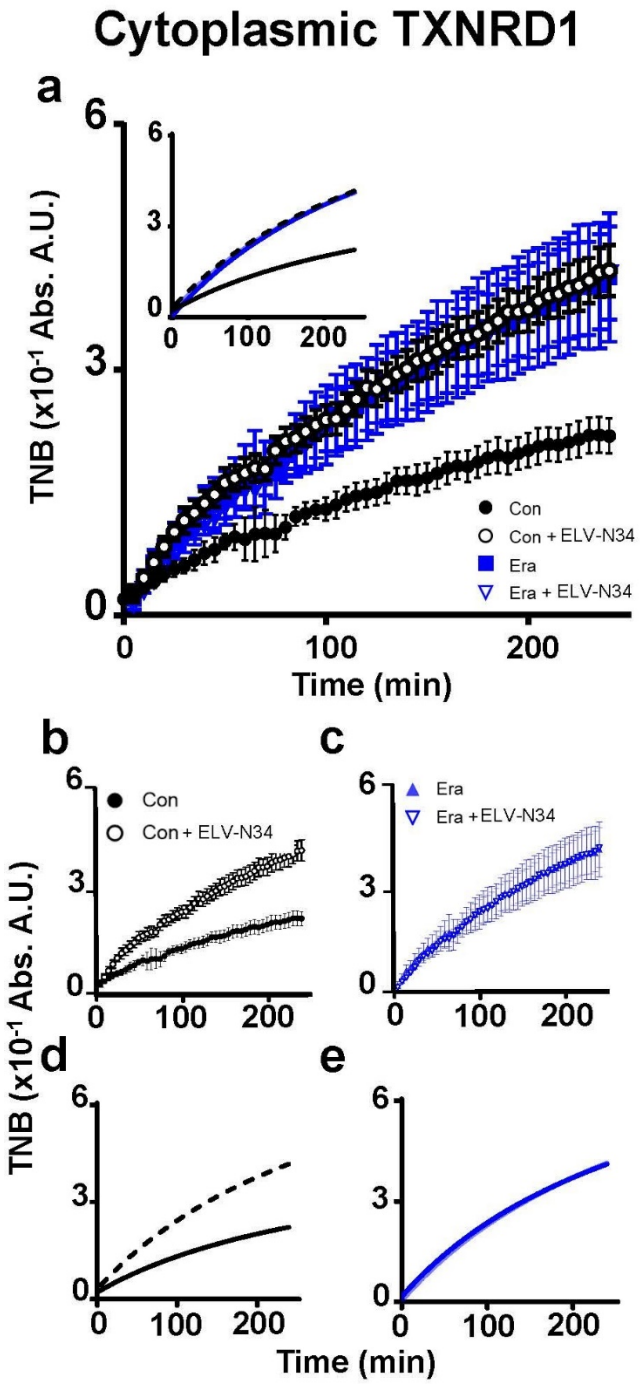

Fig. S14. Curves of Product vs. Time of the cytosolic TXNRD1. a-e, 200 nM ELV-N34 was added to the ABC cells exposed to Erastin or naïve. The activity of TXNRD1 was recorded on the cytoplasmic fraction of the cells exposed to the mentioned treatments as Product (absorbance

at 412 nm) vs. Time (min). Spureus reductase activity was ruled out using a specific inhibitor of TXNRD1. **a,** Merge curves of the four conditions. **b, c,** Mean of three observations and the bars represent the standard error of the mean for Control and Control + ELV-N34 (**b**) and UOS and UOS + ELV-N34 (**c**). **d, e,** The non-linear regression curves obtained for the data points in **b** and **c**.

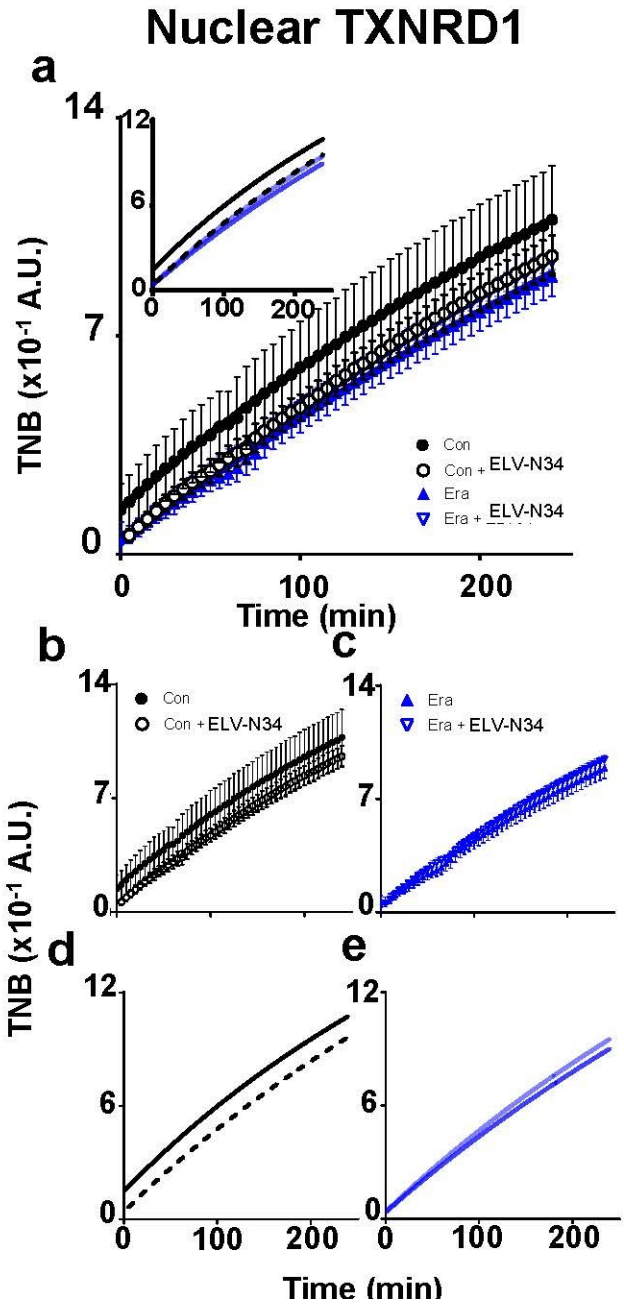

Fig. S15. Curves of Product vs. Time of the nuclear TXNRD1. a-e, 200 nM ELV-N34 was added to the ABC cells exposed to Erastin or naïve. The activity of TXNRD1 was recorded on the nuclear fraction of the cells exposed to the mentioned treatments as Product (absorbance at 412 nm) vs. Time (min). Spureus reductase activity was ruled out using a specific inhibitor of

TXNRD1. **a,** Merge curves of the four conditions. **b, c,** Mean of three observations and the bars represent the standard error of the mean for Control and Control + ELV-N34 (**b**) and UOS and UOS + ELV-N34 (**c**). **d, e,** The non-linear regression curves obtained for the data points in **b** and **c**.

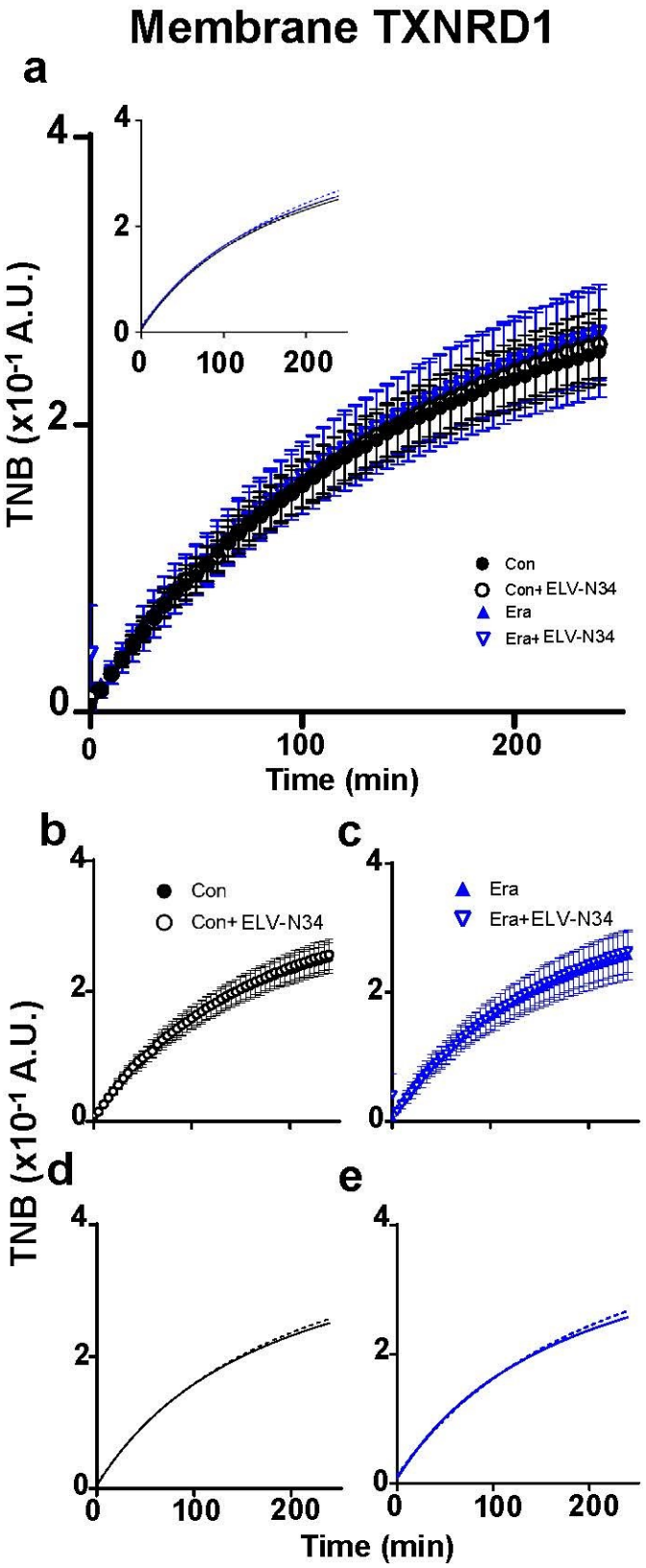
Membrane TXNRD1
a
TNB (x10-1 A.U.)
Time (min)
Con
Con+ ELV-N34
Era
Era+ ELV-N34
b
c
d
e

Fig. S16. Curves of Product vs. Time of the membrane TXNRD1. a-e, 200 nM ELV-N34 was added to the ABC cells exposed to Erastin or naïve. The activity of TXNRD1 was recorded on the membrane fraction of the cells exposed to the mentioned treatments as Product (absorbance at 412 nm) vs. Time (min). Spureus reductase activity was ruled out using a specific inhibitor of TXNRD1. **a,** Merge curves of the four conditions. **b, c,** Mean of three observations and the bars represent the standard error of the mean for Control and Control + ELV-N34 (**b**) and UOS and UOS + ELV-N34 (**c**). **d, e,** The non-linear regression curves obtained for the data points in b&c.

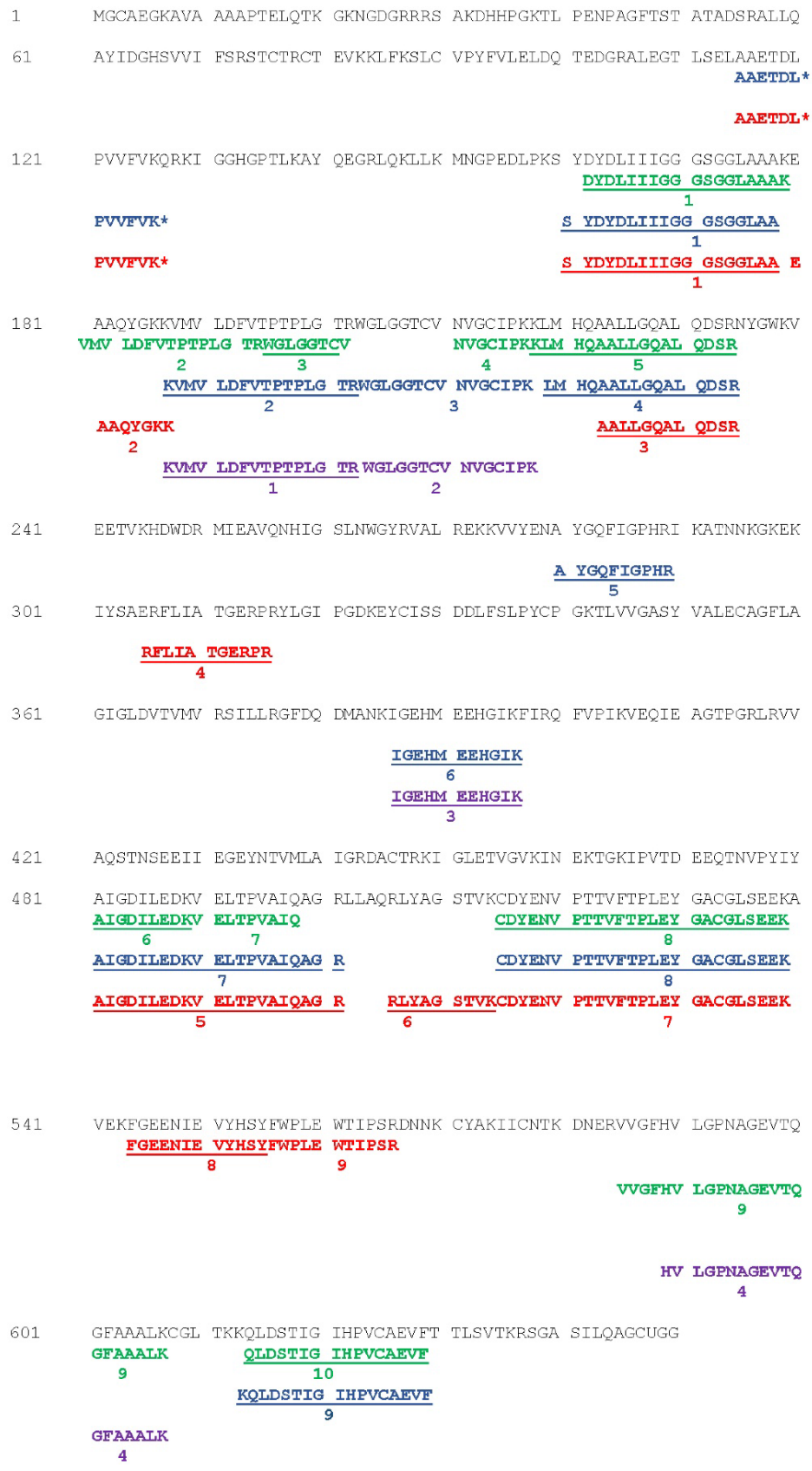
1 MGCAEGKAVA AAAPTELQTK GKNGDGRRRS AKDHHPGKTL PENPAGFTST ATADSRALLQ
61 AYIDGHSVVI FSRSTCTRCT EVKKLFKSLC VPYFVLELDQ TEDGRALEGT LSELAAETDL
AAETDL*
AAETDL*
121 PVVFVKQRKI GGHGPTLKAY QEGRLQKLLK MNGPEDLPKS YDYDLIIIGG GSGGLAAAKE
DYDLIIIGG GSGGLAAAK
1
PVVFVK*
S YDYDLIIIGG GSGGLAA
1
PVVFVK*
S YDYDLIIIGG GSGGLAA E
1
181 AAQYGKKVMV LDFVTPTPLG TRWGLGGTCV NVGCIPKKLM HQAALLGQAL QDSRNYGWKV
VMV LDFVTPTPLG TRWGLGGTCV
2 3
NVGCIPKKLM HQAALLGQAL QDSR
4 5
KVMV LDFVTPTPLG TRWGLGGTCV NVGCIPK LM HQAALLGQAL QDSR
2 3 4
AAQYGKK
2
AALLGQAL QDSR
3
KVMV LDFVTPTPLG TR
1
WGLGGTCV NVGCIPK
2
241 EETVKHDWDR MIEAVQNHIG SLNWGYRVAL REKKVVYENA YGQFIGPHRI KATNNKGKEK
A YGQFIGPHR
5
301 IYSAERFLIA TGERPRYLGI PGDKEYCISS DDLFSLPYCP GKTLVVGASY VALECAGFLA
RFLIA TGERPR
4
361 GIGLDVTVMV RSILLRGFDQ DMANKIGEHM EEHGIKFIRQ FVPIKVEQIE AGTPGRLRVV
IGEHM EEHGIK
6
IGEHM EEHGIK
3
421 AQSTNSEEII EGEYNTVMLA IGRDACTRKI GLETVGVKIN EKTGKIPVTD EEQTNVPYIY
481 AIGDILEDKV ELTPVAIQAG RLLAQRLYAG STVKCDYENV PTTVFTPLEY GACGLSEEKA
AIGDILEDKV ELTPVAIQ
6 7
CDYENV PTTVFTPLEY GACGLSEEK
8
AIGDILEDKV ELTPVAIQAG R
7
CDYENV PTTVFTPLEY GACGLSEEK
8
AIGDILEDKV ELTPVAIQAG R
5
RLYAG STVKCDYENV PTTVFTPLEY GACGLSEEK
6 7
541 VEKFGEENIE VYHSYFWPLE WTIPSRDNNK CYAKIICNTK DNERVVGFHV LGPNAGEVTQ
FGEENIE VYHSYFWPLE WTIPSR
8 9
VVGFHV LGPNAGEVTQ
9
HV LGPNAGEVTQ
4
601 GFAAALKCGL TKKQLDSTIG IHPVCAEVFT TLSVTKRSGA SILQAGCUGG
GFAAALK
9
QLDSTIG IHPVCAEVF
10
KQLDSTIG IHPVCAEVF
9
GFAAALK
4

Fig. S17. Peptides obtained from the LiP study performed with ABC cells undergoing UOS (Fig. 1 and Table S2, green), Erastin (Fig. 2 and Table S4, blue), UOS (Fig. 2 and Table S3, red), and ELV-N34; UOS + NPD1 (purple).